

Strain relaxation in InAs self-assembled quantum dots induced by a high N incorporation

J. F. Chen, C. H. Yang, Y. H. Wu, L. Chang, and J. Y. Chi

Citation: [Journal of Applied Physics](#) **104**, 103717 (2008); doi: 10.1063/1.3028235

View online: <http://dx.doi.org/10.1063/1.3028235>

View Table of Contents: <http://scitation.aip.org/content/aip/journal/jap/104/10?ver=pdfcov>

Published by the [AIP Publishing](#)

Articles you may be interested in

[Strain study of self-assembled InAs quantum dots by ion channeling technique](#)

J. Appl. Phys. **100**, 103502 (2006); 10.1063/1.2382421

[Strain relaxation and induced defects in InAsSb self-assembled quantum dots](#)

Appl. Phys. Lett. **88**, 233113 (2006); 10.1063/1.2212064

[Strain status of self-assembled InAs quantum dots](#)

Appl. Phys. Lett. **77**, 1295 (2000); 10.1063/1.1290152

[Strain relaxation and segregation effects during self-assembled InAs quantum dots formation on GaAs\(001\)](#)

Appl. Phys. Lett. **77**, 409 (2000); 10.1063/1.126992

[Strain relaxation-induced modifications of the optical properties of self-assembled InAs quantum dot superlattices](#)

J. Vac. Sci. Technol. B **18**, 1493 (2000); 10.1116/1.591411



Re-register for Table of Content Alerts

Create a profile.



Sign up today!



Strain relaxation in InAs self-assembled quantum dots induced by a high N incorporation

J. F. Chen,^{1,a)} C. H. Yang,¹ Y. H. Wu,² L. Chang,² and J. Y. Chi³

¹*Department of Electrophysics, National Chiao Tung University, Hsinchu 300, Taiwan, Republic of China*

²*Department of Materials Science and Engineering, National Chiao Tung University, Hsinchu 30010, Taiwan, Republic of China*

³*Industrial Technology Research Institute (OES/ITRI), Hsinchu 310, Taiwan, Republic of China*

(Received 1 July 2008; accepted 8 October 2008; published online 24 November 2008)

The effect of a high N incorporation in self-assembled InAs quantum dots (QDs) is investigated by analyzing the electronic and structural properties around QD region. Capacitance-voltage profiling and admittance spectroscopy shows that N incorporation into the InAs QD layer leads to drastic carrier depletion in the QD layer and neighboring GaAs layers due to the formation of a deep defect state at 0.34–0.41 eV. The signature of this defect state is similar to those defects observed in strain relaxed QDs or InGaAs/GaAs quantum wells when the InAs deposition thickness exceeds a critical thickness. Accordingly, the N incorporation might result in strain relaxation either by increasing localized strain or by inducing composition inhomogeneities, which provide nucleation sources for strain relaxation. The argument of strain relaxation is supported by transmission electron microscopy that reveals lattice misfits at the QD layer and neighboring GaAs layers. © 2008 American Institute of Physics. [DOI: 10.1063/1.3028235]

I. INTRODUCTION

Self-assembled quantum dots (QDs) (Refs. 1–19) have recently attracted a great deal of attention due to their scientific studies and promising technological applications. There is increasing interest in extending the emission wavelength for communication applications. Capping InAs QDs by a strain reducing InGaAs layer can achieve the wavelength extension¹⁶ by enlarging the dot size. Incorporating N atoms into the InGaAs cap layer can further redshift the emission by penetrating the wave function into the cap layer due to the reduction in the potential barrier of the cap layer.^{17,18} However, this wavelength extension is rather limited. N atoms can also be incorporated directly into an InGaAs QD layer to form GaInNAs QDs for achieving a long emission wavelength.¹⁹ Unfortunately, photoluminescence (PL) spectra are severely degraded at a high N content.¹⁹ This degradation is usually attributed to a formation of deep levels such as bulk²⁰ or interfacial²¹ traps observed in (In)GaAsN alloys grown on GaAs. However, the origin of these defects has not yet been established. In a previous work,²² an abnormal blueshift of the emission wavelength was observed when a high N content was incorporated into an InAs QD layer. The PL spectra became very broad and asymmetric with a very long low-energy tail extending to 1.5 μm .²² In this study, we continue this work to characterize the detailed electronic and structural properties of the QDs in order to establish the underlying reasons for the PL degradation and the abnormal N-incorporation induced blueshift. We showed that the N incorporation led to drastic carrier depletion near the QD region due to an induction of a deep defect state at 0.34–0.41 eV. The signature of this defect is similar to those states observed in strain relaxed InAs QDs and InGaAs/GaAs

quantum wells (QWs) when the InAs or the InGaAs deposition thickness exceeds a critical thickness, suggesting that the N incorporation might lead to localized strain relaxation of the QDs. This conclusion is supported by the cross-sectional transmission electron microscopy (TEM) that shows lattice misfits near the QD region. Accordingly, the abnormal PL blueshift is attributed to strain relaxation, consistent with the previous observation of a blueshift²³ when strain relaxation in InAs QDs occurs by increasing the InAs deposition thickness beyond a critical thickness.

II. EXPERIMENTS

Samples were grown on an n^+ -GaAs (100) substrate by molecular beam epitaxy in a Riber Epineat machine. An InAs QD structure consisting of a 2.4 ML (monolayer) InAs layer and a 60 Å $\text{In}_{0.15}\text{Ga}_{0.85}\text{As}$ cap layer grown at a rate of 1.86 Å/s at 480 °C, was sandwiched between two 0.3 μm thick Si-doped GaAs ($\sim 7 \times 10^{10} \text{ cm}^{-3}$) barrier layers. Indium and gallium were supplied from Knudsen cells, and As in the form of As_2 was supplied from a cracker source. N atoms were incorporated into the InAs layer using an EPI-Unibulb radio-frequency plasma source to supply active nitrogen species from ultrapure N_2 gas. Assuming the added N is completely incorporated into the InAs sublattice, we estimated the N content to be 17% from the growth rates of the InAs (0.26 Å/s) and GaAs (2.78 Å/s) layers assuming the N incorporation efficiency is similar to that in GaAsN layer.²⁴ Such a high N composition is due to the very low growth rate of the InAs QD layer for gaining a high density of the QDs. If the same N source is incorporated into a GaAs layer at a growth rate of 2.78 Å/s, the resulted N composition would be about 2%. Schottky diodes were realized by evaporating Al with a dot diameter of 1500 μm after a slight chemical etch on the sample surface.

^{a)}Electronic mail: jfchen@cc.nctu.edu.tw.

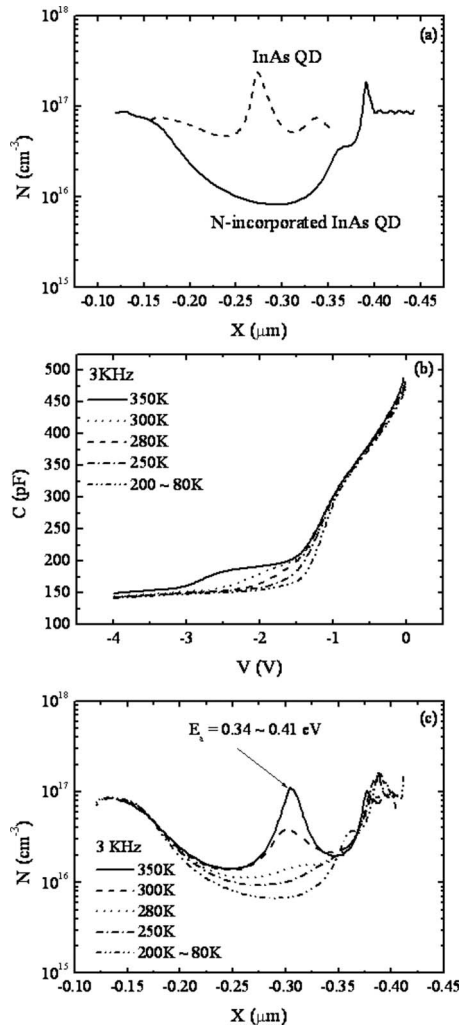


FIG. 1. (a) Depth profiles of the N-incorporated InAs QD and a reference InAs QD without N incorporation measured at 300 K and 10^5 Hz. N incorporation induces a defect state that results in drastic carrier depletion in the QD and neighboring GaAs layers. (b) Temperature-dependent C - V and (c) the corresponding depth profiles of the N-incorporated InAs QD, illustrating a C plateau (from -1.5 to -2.5 V) and a corresponding peak related to electron emission from the defect state.

III. MEASUREMENT AND RESULTS

A. Capacitance-voltage (C - V) profiling

The effect of N incorporation on the electronic properties of the QDs is illustrated in Fig. 1(a), which shows the free-electron depth profiles converted from room-temperature C - V curves at a high modulating frequency of 10^5 Hz for 2.4 ML InAs QDs with and without N incorporation. The InAs QDs (without N incorporation) shows strong electron accumulation at the QDs and nearly symmetric carrier depletion with a valley concentration of 5×10^{16} cm⁻³ on both sides of the QDs. The peak position ($0.27 \mu\text{m}$) is slightly less than the expected QD depth of $0.3 \mu\text{m}$, which is due to a slight chemical etching on the sample surface before Schottky metal evaporation. When temperature is lowered, a right shoulder (at a larger reverse bias) can be resolved from the carrier peak. The main peak and the shoulder are attributed to the depopulation of the QD excited states and the ground state, respectively. The emis-

sion time from the shoulder (QD ground state) can be resolved to yield an activation energy E_a of ~ 58 meV,²⁵ which is close to the energy difference between the ground and first-excited PL transitions. Accordingly, the shoulder is attributed to electron emission from the QD ground to the first-excited state and a subsequent tunneling to the bottom GaAs. Detailed properties of this two-stage emission process can be found elsewhere.^{15,25}

Upon N incorporation, the carrier distribution is changed to drastic carrier depletion (with a deepest valley concentration of 8×10^{15} cm⁻³) around the QD. The carrier depletion can be seen to extend far into the GaAs barrier layers. This carrier distribution suggests the presence of a deep defect state, which traps the electrons in the QD states and neighboring GaAs layers. Due to a long emission time of the defect state, the electron emission from the defect state is incapable of following the modulated frequency ($F=10^5$ Hz). Increasing temperature or lowering modulating frequency can reduce the emission time and allow for the modulation of the electrons trapped on the defect state. As shown in Figs. 1(b) and 1(c), for $T > 300$ K and at $F=3$ kHz, an additional capacitance plateau emerges from -1.5 to -2.5 V, which converts to a peak with a large full width at half maximum (FWHM) of ~ 20 nm (at 350 K). The long tail on both side of the peak in Fig. 1(c) suggests the spatial extension of the defect state into neighboring GaAs layers. Since the peak position ($0.31 \mu\text{m}$) in Fig. 1(c) represents the position of the edge of the depletion region when Fermi level intersects the defect state, the FWHM of 20 nm corresponds to an energy downward shift of about 100 meV for the Fermi level at a depth of $0.3 \mu\text{m}$, based on a simple Schottky depletion model. Thus, the defect state is considered to have a spectral broadness of about 100 meV.

B. Admittance spectroscopy

The energy position of the defect state is obtained from the activation energy of the electron emission from the defect state by performing admittance spectroscopy on the capacitance plateau (from -1.5 to -2.5 V) in Fig. 1(b). Figures 2(a)–2(c) show the conductance/frequency-frequency (G/F - F) spectra for -1.5 , -2 , and -2.5 V, respectively, measured at several temperatures as shown (with a step of 10 K). The conductance will reach a peak when frequency is comparable to the emission rate. A strong peak E_1 is seen at the three voltages and a very weak peak E_2 is seen only at -1.5 V. From their Arrhenius plots, emission energies (capture cross sections) of E_1 are determined to be 0.34 eV (4.16×10^{-16} cm²), 0.38 eV (5.74×10^{-16} cm²), and 0.41 eV (3.10×10^{-16} cm²) for -1.5 , -2 , and -2.5 V, respectively, as shown in Fig. 3. Treating the different activation energies as a spectral broadness, this defect state E_1 lies at ~ 0.38 eV with a linewidth broadness of about 70 meV, which is comparable to the value estimated from the FWHM of the peak in Fig. 1(c). Since the defect extends into the GaAs barrier layers, it is reasonable to assume that the observed emission energy is related to the GaAs conduction band. Thus, the defect state shall lie at ~ 0.38 eV below the GaAs conduction band. Kapteyn *et al.*¹⁵ estimated the con-

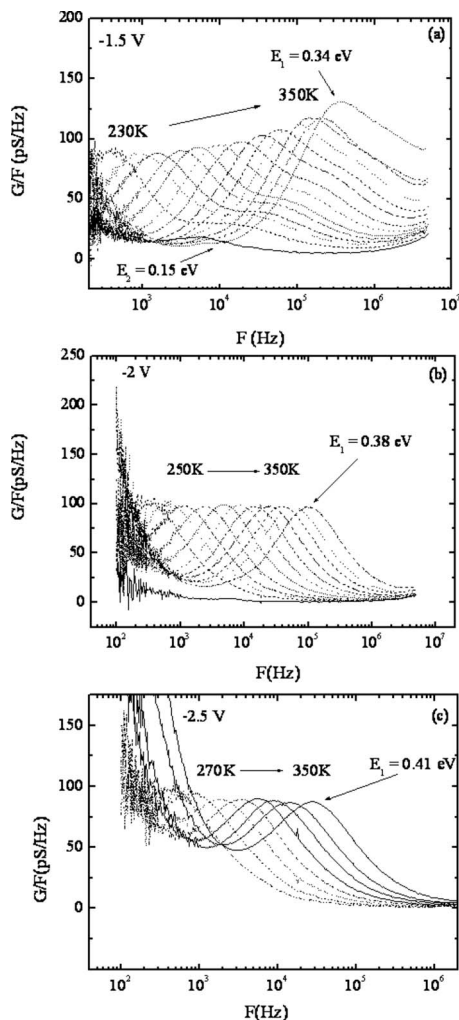


FIG. 2. G/F - F spectra of the N-incorporated InAs QD measured at (a) -1.5 V, (b) -2 V, and (c) -2.5 V, respectively. A dominant E_1 peak with 0.34 , 0.38 , and 0.41 eV can be seen for -1.5 , -2 , and -2.5 V, respectively. This peak is attributed to an emission from the N-induced defect state. Aside from this peak, the G/F spectra at -1.5 V show another weak peak E_2 with 0.15 eV, which is tentatively attributed to an emission from the QD state.

finement energy of 0.19 eV for the electron ground state (EGS) of InAs QDs emitting a wavelength close to our N-incorporated InAs QDs (~ 1.02 eV at 300 K). Taking this

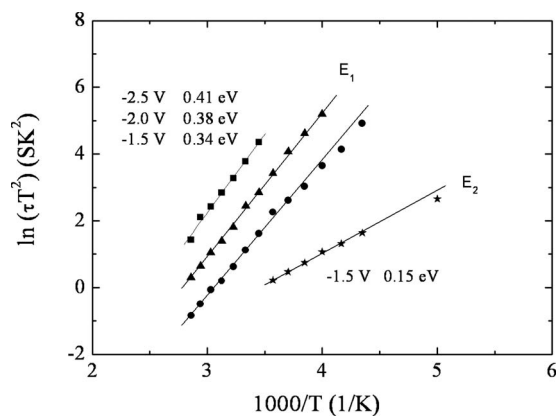


FIG. 3. Arrhenius plots of the E_1 and E_2 states observed in the G/F spectra in the N-incorporated InAs QDs.

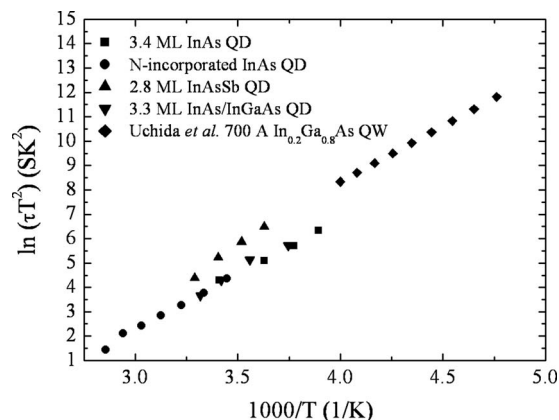


FIG. 4. Arrhenius plots of the E_1 defect state induced by N incorporation and previously observed plots of the defect states in relaxed 3.4 ML InAs QDs (Ref. 26), 3.3 ML InAs QDs with an InGaAs capping layer (Ref. 25), relaxed 2.8 ML InAsSb QDs (Ref. 27), and relaxed InGaAs/GaAs QW (Ref. 28). The comparability suggests that the E_1 defect state is associated with strain relaxation in the QDs.

energy for the EGS, the defect state would be ~ 0.19 eV below the EGS, allowing for the carrier depletion of the QDs.

As to the origin of the weak emission E_2 whose emission energy (capture cross section) is determined to be 0.15 eV (1.46×10^{-18} cm²) as shown by its Arrhenius plots in Fig. 3, it is only observed at -1.5 V and thus it is spatially confined in a very narrow QD layer. This emission is very weak and thus the experimental uncertainty for the activation energy is rather large. It could be another defect state induced by N incorporation or an electron emission from the QD state. Postgrowth thermal annealing is found to enhance the E_2 emission and diminish the E_1 emission, suggesting that annealing can remove the defect state at ~ 0.38 eV, which can in turn lead to a recovery of electrons in the QDs. Accordingly, the E_2 emission is tentatively assigned to an emission from the QD state. Our experimental data show no apparent redshift by incorporating N into the InAs QD deposition layer. This observation leads us to suspect that either the InAs band gap is not reduced by N substitution of As sublattice or the incorporated N atoms do not occupy the As sublattice. If the incorporated N atoms do not occupy the As sublattice, they are likely in defect sites. We found that a postgrowth thermal annealing can redshift the PL emission from the InGaAs cap layer, suggesting a diffusion of the incorporated N atoms into the InGaAs cap layer to form an InGaAsN cap layer during annealing. Hence, the incorporated N atoms actually enter into the InAs QDs during the growth. Thermal annealing can diffuse the N atoms to the InGaAs cap layer, leading to the recovery of free electrons in the QDs and the emission from the QD states, E_2 . Further investigation is currently underway to make further argument.

To establish the origin of the defect state E_1 (0.38 eV), Fig. 4 compares its Arrhenius plots (the solid circles) with the previously observed plots of those defects reported in relaxed 3.4 ML InAs QDs,²⁶ 3.3 ML InAs QDs with an InGaAs capping layer,²⁵ relaxed 2.8 ML InAsSb QDs,²⁷ and relaxed InGaAs/GaAs QW.²⁸ These plots are comparable,

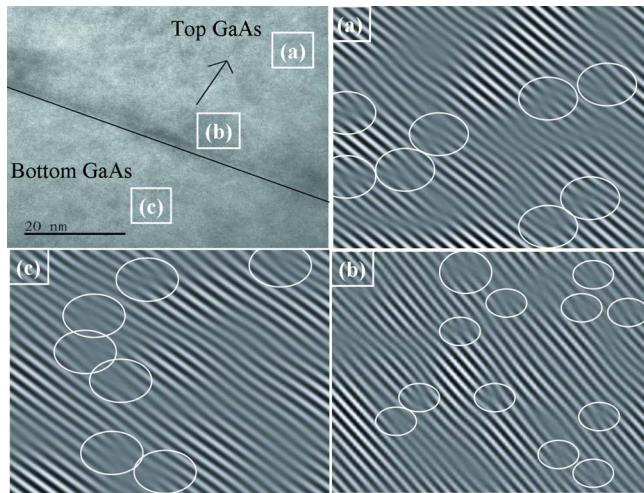


FIG. 5. (Color online) Cross-sectional TEM picture of the N-incorporated InAs QD (the top figure on the left). The wetting layer is indicated by a line for guiding the eyes. Figures indicated by (a), (b), and (c) are the Fourier transformed images for the area in the neighboring top GaAs layer, in the QD, and in the neighboring GaAs bottom layer, respectively. Significant lattice misfits can be clearly seen, as indicated by the circles.

suggesting that the defect E_1 is likely related to strain relaxation in the QDs. This comparability also suggests that the nature of the defect is only related to strain relaxation, irrelevant of QD or QW or In or Sb composition. Hence, the N incorporation might lead to strain relaxation either by increasing the strain between the QD and the GaAs barrier layers or providing nucleation sites for strain relaxation. This 0.38 eV defect state can also be detected by deep-level transient spectroscopy.²² As those defects in the above references, the peak amplitude of this defect state displays a saturation of its amplitude with increasing filling pulse duration time, suggesting a regular point-defectlike property in contrast to threading dislocations that show an unsaturated logarithmic dependence on filling pulse duration time.²⁹ This result suggests a high structural regularity for the defects induced by strain relaxation. These defects are well confined near the relaxed QD or QW region, in contrast to threading dislocations that penetrate deep into the GaAs barrier layer.^{26,27}

C. TEM characterization

To clarify whether the QDs are strain relaxed, Fig. 5 shows the cross-sectional TEM picture of the N-incorporated QD sample. A line of the QDs can be seen (the wetting layer is indicated by a line for guiding the eyes). In contrast to the QDs without N incorporation, the color contrast of QDs is unclear, and thus precise determination of dot size is difficult. A rough estimation is ~ 10 nm in height and ~ 20 nm in base width. To illustrate detailed structures, we show the Fourier transformed image in the neighboring top GaAs layer, in the QD, and in the neighboring GaAs bottom layer (indicated by (a), (b), and (c), respectively). A significant number of lattice misfits (encircled) can be seen in all three areas. Their Fourier images are similar as those previously observed in relaxed InAs QDs.³⁰ Note that no such misfits are observed in 2.4 ML thick InAs QDs without N incorpo-

ration. Although N is only incorporated during the deposition of the InAs QD layer, the misfits are observed in the neighboring GaAs barrier layers and in the intervening GaAs region between the QDs. These misfits do not propagate deep into the GaAs barrier layers; they are confined around the QD of about 60 nm in total thickness. This spatial distribution is consistent with that of the 0.38 eV defect state, which displays long tails on both sides of the emission peak (at 350 K) as shown in Fig. 1(c). These misfits act as the electron-trapping defect state, and since most of the misfits are located in the GaAs material (rather than in the QDs), the observed electron emission process should be relative to the GaAs conduction band, as assumed for the 0.38 eV defect state above. These misfits are well confined near the QD layer, rather than penetrating deep into the top or bottom GaAs layers. They have much higher structural and electronic regularity than threading dislocations, consistent with the defect states associated with lattice misfits.^{25,27} These results support that N incorporation into the InAs QD layer results in strain relaxation in the QDs. This could occur either by increasing the strain between QD and GaAs layers or induced defects, which provide nucleation sites for strain relaxation. However, as in GaAs, N substitution of As in InAs is expected to decrease lattice constant, which would decrease the lattice mismatch between the QD layer and the GaAs layers and reduce strain. Hence, we tend to exclude the strain increase as the cause for relaxation. On the other hand, due to a large difference between the radii of As and N atoms, a high N incorporation into As-related alloys often leads to significant composition fluctuation or even phase separation,¹⁹ although the lattice mismatch with the GaAs layers is decreased. Thus, the composition inhomogeneity caused by N incorporation is attributed to the cause for strain relaxation of the QDs. The composition inhomogeneity may lead to the very long low-energy tail up to $1.5 \mu\text{m}$ (Ref. 22) observed in the PL spectra. The carrier depletion caused by the misfit related defect state can lead to a large conduction-band protrusion in the vicinity of the QD, preventing the photogenerated carriers from entering the QD layer and degrading the PL emission.

Strain relaxation in the QDs can cause blueshift of the PL emission. In the previous work,²³ when the InAs deposition thickness is below the critical thickness (~ 3 ML) for strain relaxation, increasing InAs deposition thickness can redshift the emission due to an increase in dot size. However, when the InAs deposition thickness is further increased from 2.7 to 3.06 ML, the PL emission undergoes an abnormal blueshift of 68 meV (from 1310 to 1223 nm at 300 K). This blueshift is accompanied with the generation of lattice misfits and the 0.38 eV defect state. Hence, the blueshift is explained by the relief of built-in strain. Before relaxation, due to the underlying GaAs layer, the InAs QD is compressed perpendicular to the growth direction, giving rise to tensile strain in the QDs along the growth direction. Since the dot height is much smaller than the lateral dimension, the size-confinement effect and the related PL emission shift are dominated by the lattice constant along the growth direction. The tensile strain along the growth direction can extend the dot height, which extends the emission wavelength. Strain

relaxation relieves this strain and causes a blueshift. This can explain the observed blueshift from 1215 to 1060 nm (at 50 K) when N is incorporated into the InAs layer.²²

IV. CONCLUSIONS

A high N incorporation into the InAs QD layer is shown to change the carrier distribution from accumulation to drastic depletion near the QD. When temperature is increased and frequency is lowered, a broad peak emerges from the depletion region. This peak is interpreted as an electron emission from a deep defect state. Admittance spectroscopy reveals an emission energy of ~ 0.38 eV for this defect state. Judging from its Arrhenius plots, this defect state is likely the state previously observed in strain relaxed QDs or relaxed InGaAs/GaAs QW, suggesting that N incorporation might result in strain relaxation in the QDs. This argument is confirmed by the TEM data that clearly show lattice misfits in the QD layer and the neighboring GaAs layers. From their similar spatial distribution, the 0.38 eV defect state is attributed to the lattice misfits. Hence, N incorporation results in strain relaxation in the QDs by the accommodation of the lattice misfits, which act as electron-trapping centers to deplete the electrons in the QDs.

ACKNOWLEDGMENTS

The authors would like to thank Dr. R. S. Hsiao for sample preparation, the National Science Council of the Republic of China, Taiwan for financially supporting this research under Contract No. NSC-97-2112-M-009-014-MY3, and the MOE, ATU program.

¹F. Heinrichsdorff, M.-H. Mao, N. Kirstaedter, A. Krost, and D. Bimberg, *Appl. Phys. Lett.* **71**, 22 (1997).

²H. Saito, K. Nishi, and S. Sugou, *Appl. Phys. Lett.* **73**, 2742 (1998).

³D. J. Eaglesham and M. Cerullo, *Phys. Rev. Lett.* **64**, 1943 (1990).

⁴D. Leonard, K. Pond, and P. M. Petroff, *Phys. Rev. B* **50**, 11687 (1994).

⁵S. Guha, A. Madhukar, and K. C. Rajkumar, *Appl. Phys. Lett.* **57**, 2110 (1990).

⁶J. M. Moison, F. Houzay, F. Barthe, and L. Leprince, *Appl. Phys. Lett.* **64**, 196 (1994).

⁷D. J. Bottomley, *Appl. Phys. Lett.* **72**, 783 (1998).

⁸C. W. Snyder, J. F. Mansfield, and B. G. Orr, *Phys. Rev. B* **46**, 9551 (1992).

⁹D. Leonard, M. Krishnamurthy, C. M. Reaves, S. P. Denbaars, and P. M. Petroff, *Appl. Phys. Lett.* **63**, 3203 (1993).

¹⁰H. Shoji, K. Mukai, N. Ohtsuka, M. Sugawara, T. Uchida, and H. Ishikawa, *IEEE Photonics Technol. Lett.* **7**, 1385 (1995).

¹¹G. Yusa and H. Sakaki, *Electron. Lett.* **32**, 491 (1996).

¹²N. Yokoyama, S. Muto, K. Imamura, M. Takatsu, T. Mori, Y. Sugiyama, Y. Sakuma, H. Nakao, and T. Adachihiro, *Solid-State Electron.* **40**, 505 (1996).

¹³Y. Arakawa and H. Sakaki, *Appl. Phys. Lett.* **40**, 939 (1982).

¹⁴J. C. Campbell, D. L. Huffaker, H. Deng, and D. G. Deppe, *Electron. Lett.* **33**, 1337 (1997).

¹⁵C. M. A. Kapteyn, F. Heinrichsdorff, O. Stier, R. Heitz, M. Grundmann, and P. Werner, *Phys. Rev. B* **60**, 14265 (1999).

¹⁶N. Tatebayashi, M. Nishioka, and Y. Arakawa, *Appl. Phys. Lett.* **78**, 3469 (2001).

¹⁷V. C. Ustinov, A. Y. Egorov, V. A. Odnoblyudov, N. V. Kryzhanovskaya, Y. G. Musikhin, A. F. Tsatsulnikov, and Z. I. Alferov, *J. Cryst. Growth* **251**, 388 (2003).

¹⁸A. Yu. Egorov, D. Bedarev, D. Bernklau, G. Dumitras, and H. Riechert, *Phys. Status Solidi B* **224**, 839 (2001).

¹⁹M. Sopanen, H. P. Xin, and C. W. Tu, *Appl. Phys. Lett.* **76**, 994 (2000).

²⁰R. J. Kaplar, S. A. Ringel, S. R. Krutz, J. F. Klem, and A. A. Allerman, *Appl. Phys. Lett.* **80**, 4777 (2002).

²¹P. Krispin, S. G. Spruytte, J. S. Harris, and K. H. Ploog, *J. Appl. Phys.* **88**, 4153 (2000).

²²J. F. Chen, R. S. Hsiao, P. C. Hsieh, Y. J. Chen, Y. P. Chen, J. S. Wang, and J. Y. Chi, *J. Appl. Phys.* **98**, 113525 (2005).

²³J. F. Chen, R. S. Hsiao, Y. P. Chen, J. S. Wang, and J. Y. Chi, *Appl. Phys. Lett.* **87**, 141911 (2005).

²⁴J. S. Wang, R. S. Hsiao, G. Lin, K. F. Lin, H. Y. Lin, C. M. Lai, L. Wei, C. Y. Liang, J. Y. Chi, J. F. Chen, and V. M. Ustinov, *J. Vac. Sci. Technol. B* **22**, 2663 (2004).

²⁵J. F. Chen, R. S. Hsiao, C. K. Wang, J. S. Wang, and J. Y. Chi, *J. Appl. Phys.* **98**, 013716 (2005).

²⁶Y. S. Wang, J. F. Chen, P. Y. Wang, and X. J. Guo, *Appl. Phys. Lett.* **77**, 3027 (2000).

²⁷J. F. Chen, R. S. Hsiao, W. D. Huang, Y. H. Wu, L. Chang, J. S. Wang, and J. Y. Chi, *Appl. Phys. Lett.* **88**, 233113 (2006).

²⁸Y. Uchida, H. Kakibayashi, and S. Goto, *J. Appl. Phys.* **74**, 6720 (1993).

²⁹T. Wosinski, *J. Appl. Phys.* **65**, 1566 (1989).

³⁰J. F. Chen, Y. Z. Wang, C. H. Chiang, R. S. Hsiao, Y. H. Wu, L. Chang, J. S. Wang, T. W. Chi, and J. Y. Chi, *Nanotechnology* **18**, 355401 (2007).